THE AMERICAN SOCIETY OF MECHANICAL ENGINEERS
345 E. 47th St., New York, N.Y. 10017

94-GT-250

INTERACTION BETWEEN INLET BOUNDARY LAYER, TIP-LEAKAGE AND SECONDARY FLOWS IN A LOW-SPEED TURBINE CASCADE

J. K. K. Chan, M. I. Yaras, and S. A. Sjolander
Department of Mechanical and Aerospace Engineering
Carleton University
Ottawa, Ontario, Canada

ABSTRACT

An experiment has been conducted in a large-scale linear turbine cascade to examine the interaction between the inlet endwall boundary layer, tip-leakage and secondary flows. Detailed flow field measurements have been made upstream and downstream of the blade row for two values of inlet boundary layer thickness (δ^*/c of about 0.015 and 0.04) together with three values of tip clearance (gap heights of 0.0, 1.5 and 5.5 percent of blade chord). In the downstream plane, the total pressure deficits associated with the tip-leakage and secondary flows were discriminated by examining the sign of the streamwise vorticity. For this case, the streamwise vorticity of the two flows have opposite signs and this proved an effective criterion for separating the flows despite their close proximity in space. It was found that with clearance the loss associated with the secondary flow was substantially reduced from the zero clearance value, in contradiction to the assumption made in most loss prediction schemes. Further work is needed, notably to clarify the influence of relative tip-wall motion which in turbines reduces the tip-leakage flow while enhancing the secondary flow.

NOMENCLATURE

c = blade chord length
c_x = blade axial chord length
C_D = discharge coefficient for the tip gap
$C_L = \dfrac{L}{\frac{1}{2}\rho V_m^2 c}$ = blade lift coefficient
$C_P = \dfrac{P-P_{CL}}{\frac{1}{2}\rho V_{CL}^2}$ = static pressure coefficient
$C_{P_O} = \dfrac{P_O-P_{O,CL}}{\frac{1}{2}\rho V_{CL}^2}$ = total pressure coefficient
C_{P_O}'' = mass-averaged total pressure coefficient
h = span
$H_x = \dfrac{\delta_x^*}{\theta_x}$ = boundary layer shape factor
L = lift force
m_{REF} = reference passage mass flow rate at the inlet
P = static pressure
P_O = total pressure
$Re = \dfrac{\rho V_{CL} c}{\mu}$ = Reynolds number based on blade chord
s = streamwise co-ordinate
S = blade spacing
t_{MAX} = blade maximum thickness
V = velocity
V_e = velocity at the boundary layer edge
x,y,z = co-ordinates in axial, pitchwise and spanwise directions
x' = co-ordinate in chordwise direction
y' = local pitchwise co-ordinate
$Y = \dfrac{P_{O,1}-P_{O,2}}{\frac{1}{2}\rho V_2^2}$ = total pressure loss coefficient
α = flow angle, measured from the axial direction
β = blade metal angle, measured from the axial direction
γ = blade stagger angle
δ = boundary layer thickness

Presented at the International Gas Turbine and Aeroengine Congress and Exposition
The Hague, Netherlands — June 13–16, 1994

δ_x^* = $\int_0^\delta (\frac{V_{x_e}}{V_e} - \frac{V_x}{V_e}) dz$ = boundary layer displacement thickness

θ_x = $\int_0^\delta (\frac{V_{x_e}}{V_e} - \frac{V_x}{V_e}) \frac{V_x}{V_e} dz$ = boundary layer momentum thickness

μ = dynamic viscosity
ρ = density
τ = tip gap height
ω = vorticity
ω' = non-dimensional vorticity $(\frac{\omega c}{V_1})$

Subscripts

CL = centreline value at inlet
e = boundary layer edge value
m = mean value through blade row
x,y,z = components in axial, pitchwise and spanwise directions
s = component in the streamwise direction
1,2 = cascade inlet and outlet

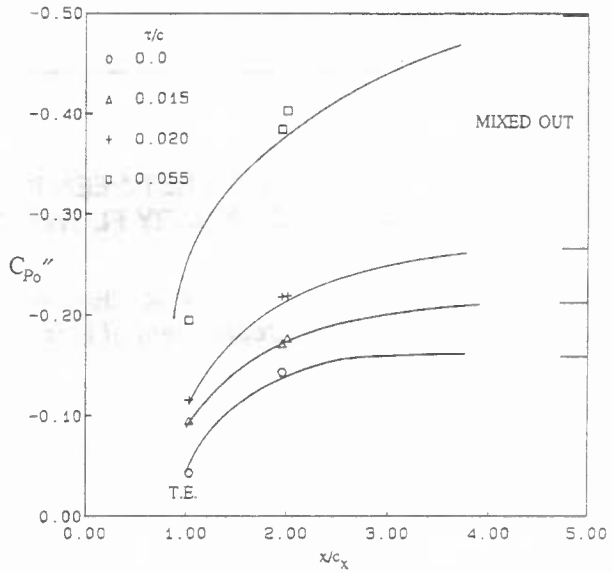

Fig. 1. Variation of Total Pressure Coefficient with Downstream Distance (from Yaras and Sjolander, 1989).

INTRODUCTION

The secondary and tip-leakage flows in turbines have been the subject of extensive research in recent years. In the tip region, these two flows are in close proximity and strongly interactive. Despite this, most existing studies have considered the flows separately and made few attempts to clarify their inter-relationship. This is a natural consequence of the difficulty in separating the two flows in experimental measurements.

Most previous references to the interaction between the secondary and tip-leakage flows have been tentative and often qualitative. From flow visualization studies, Sjolander and Amrud (1987) concluded that a significant portion of the incoming tip-wall boundary layer fluid passes through the tip gap near the leading edge. This qualitative result was later quantified from the tip-gap measurements of Yaras et al. (1989) who concluded that for their flow about one third of the original endwall boundary layer ended up in the tip-gap flow. Yamamoto (1988) concluded from cascade observations that the strength of the interaction between the tip-leakage and secondary flows increases with increased flow turning and larger clearance size. The work of Dishart and Moore (1990) and Yaras and Sjolander (1992) showed that the losses associated with the formation and diffusion of the tip-leakage vortex are closely approximated by the tip-leakage kinetic energy carried by the normal component of the tip-gap velocity. It is unclear, however, to what extent this relation is affected by the relatively low energy boundary layer fluid entering the tip gap.

There is some evidence in the available literature that, in the absence of tip clearance, the secondary losses are not sensitive to the amount of total pressure deficit in the inlet wall boundary layer. However, it is not known whether this remains true for nonzero tip clearance. It is also unclear how the secondary losses are affected by the presence of tip leakage.

Most schemes for estimating the losses in axial-flow turbines linearly superimpose the losses due to the various loss mechanisms. Thus, for example, the secondary losses in the tip region are assumed to be the same regardless of the size of the tip clearance. To obtain the tip-clearance losses from measurements, the secondary losses measured at zero clearance are subtracted from the total losses measured with clearance. The measurements of Yaras and Sjolander (1989) indicated some physical inconsistencies in this approach. Figure 1 (reproduced from Yaras and Sjolander) shows the variation with downstream distance of the mass-averaged total pressure coefficients for a range of clearances. It is seen that the secondary losses, as obtained at zero clearance, increase substantially with downstream distance. This is a well known effect and is mainly the result of the additional losses due to the mixing out of the secondary vortex. With clearance the total losses likewise rise with downstream distance. However, the observed "tip-clearance loss", that is the additional loss over and above the observed secondary loss, is seen to be reasonably constant with downstream distance, particularly for the smaller clearances. Thus, the conventional decomposition of the losses implies that the secondary losses continue to increase for some distance downstream while the tip-leakage losses remain essentially constant. This is clearly not reasonable physically. The tip-leakage flow, like the secondary flow, consists of a vigorous vortex which mixes rapidly with the surrounding flow. One would therefore expect both types of flow to experience significant additional losses downstream of the

blade row. Thus, the assumption of constant secondary loss regardless of the clearance is not consistent with the expected physics.

The present study attempts to shed some light on these issues based on measurements made in a linear turbine cascade for three clearance sizes and two inlet tip-wall boundary layer thicknesses.

EXPERIMENTAL APPARATUS AND PROCEDURES

Test Section

The experiments were carried out in the cascade test section shown schematically in Figure 2. It is described in detail in earlier papers (e.g. Sjolander and Amrud, 1987). A summary of pertinent geometric information for the cascade is given in Figure 3. The test cascade represents the tip section of a low-pressure turbine blade of fairly recent design. The tested configuration has slightly different stagger and solidity than the actual turbine. This has resulted in somewhat more forward-loaded blades compared to the engine application. The blade also has rather low turning for a turbine. As a result, the secondary flow would be expected to be somewhat weak, which is a slight disadvantage for the present purposes.

Clearance sizes of 0, 1.5 and 5.5 percent of the blade chord were tested. The adjustment of the tip clearance was realised by inserting shims between the side walls and the tip-wall window, beginning about 2.5 axial chord lengths upstream of the leading edge plane.

The circular inlet of the circular-to-rectangular transition section shown in Figure 2 was attached to the outlet of an open-jet wind tunnel. As mentioned, experiments were performed for two values of tip-wall boundary layer thickness at the cascade inlet. The relatively thin boundary layer was obtained by allowing the boundary layer to develop naturally in the transition section. To obtain a thicker inlet boundary layer on the tip wall, a sawtooth device was installed at the inlet of the transition section. It consisted of seven triangular teeth and extended over a 100° portion of the inlet circumference. The circumferential extent of the sawtooth and the distribution of tooth size along its length were determined by trial and error to retain pitchwise flow uniformity at the cascade inlet while thickening the tip-wall boundary layer.

For tests with the thicker tip-wall boundary layer, the back-wall boundary layer was bled off through a pitchwise row of holes drilled at 30° to the flow direction and located 1.13 axial chord length upstream of the leading edge plane. This reduced the secondary flows in the inner half of the blade passage, eliminating the potential for interaction between the secondary flows developing in the inner and outer halves of the passage.

Instrumentation and Data Acquisition

The outer half of the centre blade in the cascade is instrumented with 14 chordwise rows of static pressure taps, each row comprising of 37 pressure-side and 36 suction-side taps. An accuracy of ±0.02 is estimated for the measured blade static pressure coefficients.

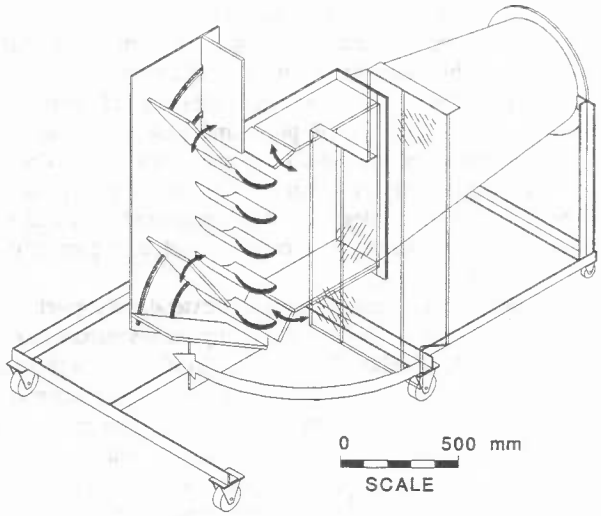

Fig. 2. Schematic of Tip-Leakage Test Section.

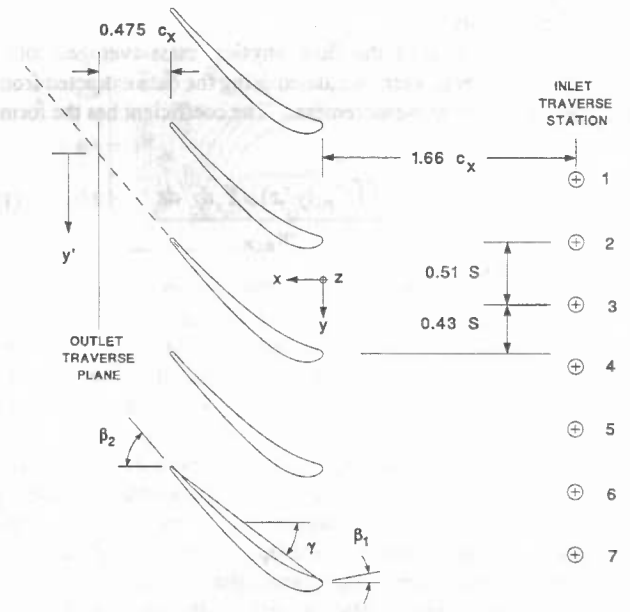

CHORD LENGTH, c	:	250 mm
AXIAL CHORD LENGTH, c_x	:	199 mm
BLADE SPAN, S	:	150 mm
BLADE SPAN, h	:	203 mm
STAGGER ANGLE,	:	37.2 ± 0.2 deg.
BLADE INLET ANGLE, β_1	:	11.1 ± 0.2 deg.
BLADE OUTLET ANGLE, β_2	:	49.6 ± 0.2 deg.

Fig. 3. Cascade Geometry and Measurement Locations.

A seven-hole pressure probe was used in the non-nulling mode for the measurements of the flow 0.475 axial chord length downstream of the blades. The probe is of 2.4 mm diameter and 60 degrees apex angle at the conical tip. For the measurements, the probe axis was aligned with the exit metal angle of the blades

and was traversed in the spanwise and pitchwise directions by means of a motorized traversing gear. The probe position is estimated to be accurate to within ±0.25 mm in all three coordinate directions. The probe was calibrated in 5 degrees steps through all combinations of pitch and yaw angles up to 50 degrees of misalignment relative to the probe axis. The flow angles extracted from the calibration curves are estimated to be accurate to within ±2 degrees. The measured total and static pressures are estimated to be accurate to within ±5 percent of the local dynamic pressure.

The downstream measurement plane extended one pitch and 60 percent of the span. This ensured complete measurement of the tip-leakage and secondary flows as well as the blade wakes in the outer part of the blade passage. A spacing of 5 percent of the blade span was chosen for the data points in the measurement plane. This provided satisfactory resolution of the flow.

All pressures were measured with capacitive-type pressure transducers. The analog output of the transducers was converted to digital form, with 12 bit resolution, using a data acquisition system controlled by a microcomputer.

Data Reduction

For interpretation of the flow physics, mass-averaged total-pressure coefficients were calculated using the data extracted from the seven-hole-probe measurements. The coefficient has the form:

$$C_{Po}{}'' = \frac{\iint C_{Po}(y',z)\,\rho\,V_x\,dy'\,dz}{m_{REF}} \tag{1}$$

where m_{REF} is the reference mass flow rate measured over one pitch and 60 percent of the span at inlet to the cascade. For zero clearance with thick tip-wall boundary layer at the inlet and for nonzero clearances, the mass flow rates measured in the downstream plane were found to be 5 to 10 percent less than this reference mass flow rate. This indicates that the full extent of the inlet streamtube was not included in the downstream measurement plane. The mass flow deficit in the measurement plane is believed to be due to the blockage effect of the tip-leakage and secondary-flow structures near the tip wall in the blade passage. The spanwise expansion of the stream tube due to these structures would be expected to take place away from the blade surfaces and thus not to affect the spanwise distribution of the profile losses. Hence, it is reasonable to assume that the mass flow rate not accounted for is free stream fluid.

The mass-averaged total-pressure coefficient at the inlet was calculated using pitot probe data and is estimated to be accurate within ±0.01. Based on repeatability tests and the established accuracy of the seven-hole pressure probe, the mass-averaged total-pressure coefficients in the downstream measurement plane are estimated to be accurate within ±0.02.

The x and y components of vorticity in the downstream measurement plane were obtained using,

$$\omega_x = \frac{\partial V_z}{\partial y} - \frac{\partial V_y}{\partial z} \tag{2}$$

$$\omega_y = \frac{1}{V_x}\left[V_y\,\omega_x + \frac{1}{\rho}\frac{\partial P_o}{\partial z}\right] \tag{3}$$

The expression for the y component of vorticity was derived from the momentum equation in the z direction under the assumptions of steady, incompressible flow and negligible viscous forces. Use of this expression allowed the evaluation of both vorticity components from measurements made in a single plane parallel to the y-z plane. The validity of this approximate method was verified by Yaras and Sjolander (1990). The accuracy of the vorticity components calculated in this fashion, nondimensionalized by the blade chord and inlet centreline velocity, is conservatively estimated to be within 10 percent of the actual value. The streamwise vorticity, taken as the component of vorticity in the primary flow direction, is then obtained from

$$\omega_s = \omega_x \cos\alpha - \omega_y \sin\alpha \tag{4}$$

where α is the primary flow direction at midspan measured relative to the axial direction.

EXPERIMENTAL RESULTS

Operating Conditions

All measurements were made at a blade Reynolds number of 4.3×10^5 ±2 percent based on the undisturbed inlet velocity and blade chord. The inlet velocity was about 30 m/s so that conditions were essentially incompressible. The turbulence intensity at the cascade inlet was 1.5 percent.

Tests were performed for three clearance sizes of 0.0, 1.5 and 5.5 percent of the blade chord and two tip-wall boundary layer thicknesses. The boundary layer velocity profiles were determined from pitot-probe traverses made 0.84 axial chord lengths upstream of the leading edge plane. The static pressure was measured on the tip wall at the same axial location. The resulting integral parameters are given in Table 1. As evident from these results, the thickness of the tip-wall boundary layer is increased by a factor of roughly three by the sawtooth. A slight increase in the boundary layer thickness when opening the tip clearance is also apparent. The latter is caused by the small ramp created between the fixed and moveable portions of the tip-wall as the tip clearance is opened.

The pitchwise uniformity of the inlet flow was verified through pitot-probe traverses made 1.66 axial chord lengths upstream of the leading-edge plane. Establishing this uniformity for the thicker tip-wall boundary layer required a number of iterations on the sawtooth geometry; Figure 4 shows three sample velocity profiles spanning slightly more than two blade pitches upstream

Table 1. Boundary Layer Parameters at Cascade Inlet.

	CLEARANCE		
τ/c	0.0	0.015	0.055
τ (mm)	0.0	3.8	13.7
	THIN INLET BOUNDARY LAYER		
δ^*_X (mm)	2.9	4.6	3.9
θ_X (mm)	2.2	3.3	3.0
H_X	1.3	1.4	1.3
	THICK INLET BOUNDARY LAYER		
δ^*_X (mm)	9.3	9.2	11.0
θ_X (mm)	7.7	7.7	8.7
H_X	1.2	1.2	1.2

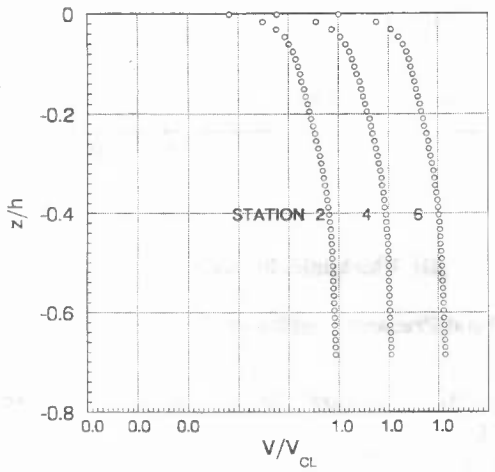

Fig. 4. Inlet Velocity Profiles for Thick Tip-Wall Boundary Layer.

of the middle blade (the traverse locations are indicated on Figure 3).

Measurement of the Downstream Flow for Zero Tip Clearance

Figure 5 shows the total pressure distribution in the downstream measurement plane for zero clearance and with thin and thick tip-wall boundary layers. A larger region of total pressure deficit is evident with increasing boundary layer thickness.

To quantify the actual change in secondary loss through the blade row the results were mass averaged. The profile losses

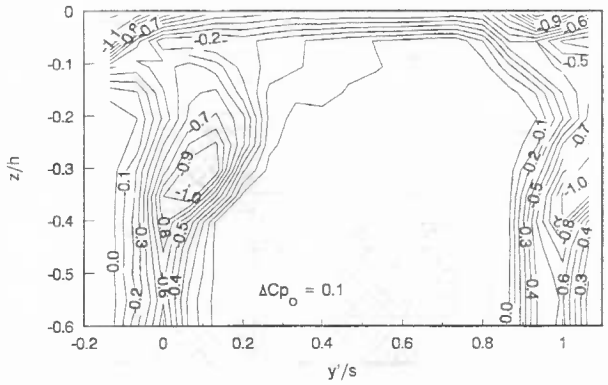

(i) Thin inlet boundary layer.

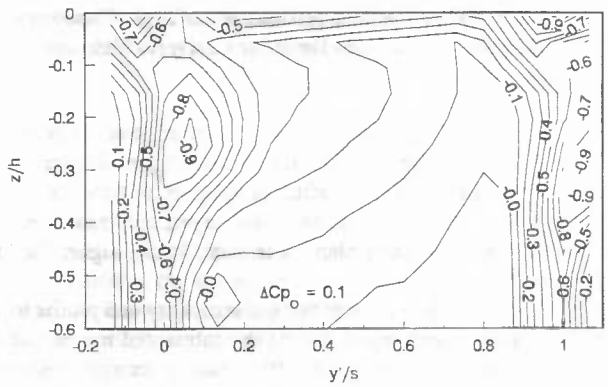

(ii) Thick inlet boundary layer.

Fig. 5. Total-Pressure Coefficient Contours for $\tau/c = 0.0$.

were calculated by mass averaging the total pressure deficit of the flow at midspan. With the present blade aspect ratio of 0.812, the secondary flows near the endwalls are likely to affect the two-dimensionality of the flow at midspan. Rodger et al (1992) examined in some detail the influence of the degree two dimensionality on the measured midspan profile losses. For axial velocity ratios larger than 1.0, which would be the case in the present work, they found a relatively small effect on the midspan profile loss. This profile loss was assumed to apply across the full blade span. The mass-averaged inlet losses were obtained by integrating the pitot-probe data obtained 0.84 axial chord lengths upstream of the leading-edge plane. The secondary losses were then calculated by subtracting the profile and inlet losses from the mass-averaged losses measured in the downstream plane. The resulting breakdown of the components, expressed as total pressure coefficients, is given in Figure 6.

The mass-averaged total pressure coefficient at the inlet is seen to be slightly positive for the thin boundary layer. This is due to

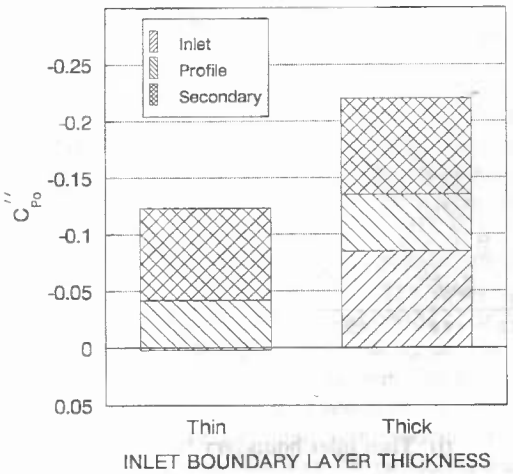

Fig. 6. Total Pressure Coefficients for Zero Clearance - Variation with Inlet Boundary Layer Thickness.

a small nonuniformity in the free stream total pressure at the cascade inlet. The centreline total pressure, which is used as the reference total pressure, is slightly lower than the values closer to the endwalls. For the thin boundary layer, the mass-averaged total pressure in the inlet plane is in fact slightly higher than the centreline value.

From Figure 6 it is evident that the secondary and profile losses remain virtually unchanged despite the substantial increase in the inlet boundary layer thickness. This result is in agreement with the cascade data compiled by Sharma and Butler (1987). The secondary loss mechanisms in the blade passage are quite complex and are not yet fully understood. There appear to be two particularly important sources of loss (Denton, 1993): the losses produced in the very thin, "new" endwall boundary layer that develops on the wall in the blade passage downstream of the separation line for the passage vortex; and the dissipation within the passage vortex itself (Denton, 1993). The entropy generation due to the former mechanism depends on the velocity field near the endwall. The viscous dissipation in the passage vortex should scale on the secondary kinetic energy carried by the secondary flow (Gregory-Smith, 1982; Sieverding, 1985). The results of the current work suggest that the effect of the inlet boundary layer thickness on these aspects of the passage flow is small.

Another loss mechanism for the secondary flow is the mixing-out of the inlet boundary layer in the passage. While this loss may be somewhat amplified by the secondary flows in the passage, it is likely to depend dominantly upon the extent of the flow nonuniformity at the inlet, i.e. the inlet boundary layer thickness. In the current work, the absence of a notable change in the secondary losses, despite the significant change in the inlet boundary layer thickness, suggests that this loss mechanism accounts for only a small portion of the secondary loss generated in the blade passage.

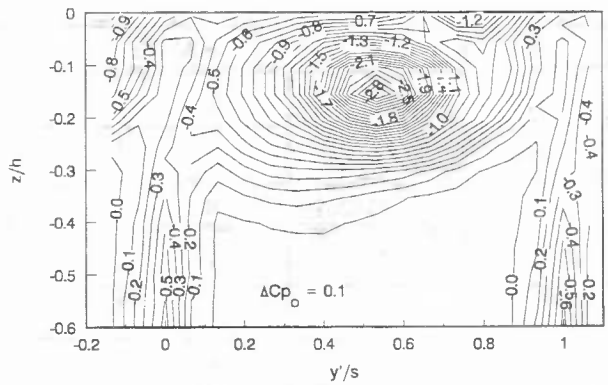

(i) Thin inlet boundary layer.

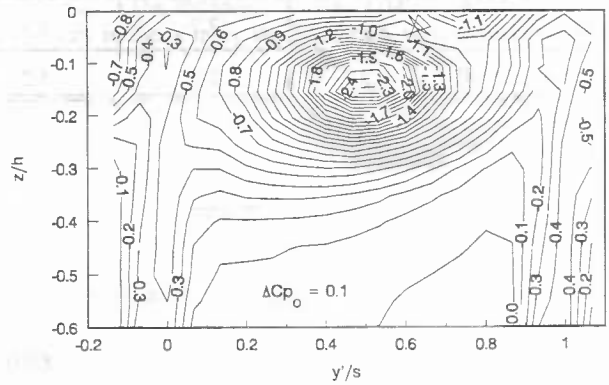

(ii) Thick inlet boundary layer.

Fig. 7a. Total Pressure Coefficient Contours for τ/c = 0.055.

Measurement of the Downstream Flow for Nonzero Tip Clearance

Figures 7(a) and 7(b) show the total pressure and streamwise vorticity distributions in the downstream measurement plane for a clearance size of 5.5 percent of the blade chord. Results are presented for both thin and thick boundary layers at the inlet.

Due to their opposite sense of rotation, the passage and tip-leakage vortices are easily discriminated on the streamwise vorticity plots. For the selected coordinate system the tip-leakage vortex contains negative streamwise vorticity. This vortex is seen to dominate the outer half of the passage for both boundary layer thicknesses. The passage vortex is located beneath the tip-leakage vortex, partially wraps itself around the tip-leakage vortex and is of considerably smaller size.

Comparison of the results for thick and thin inlet boundary layers shows little change in the size of the flow structures. A slight reduction in the peak vorticity at the centres of both vortices is apparent with increasing inlet boundary layer thickness.

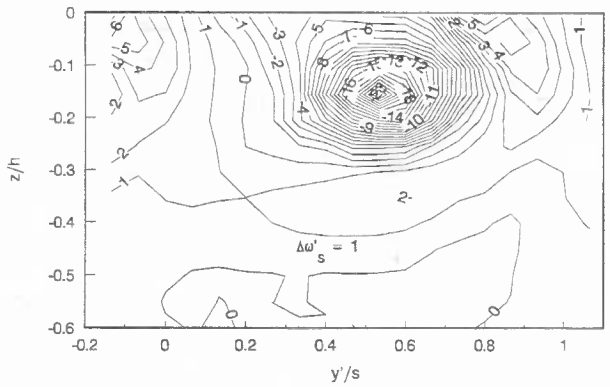

(i) Thin inlet boundary layer.

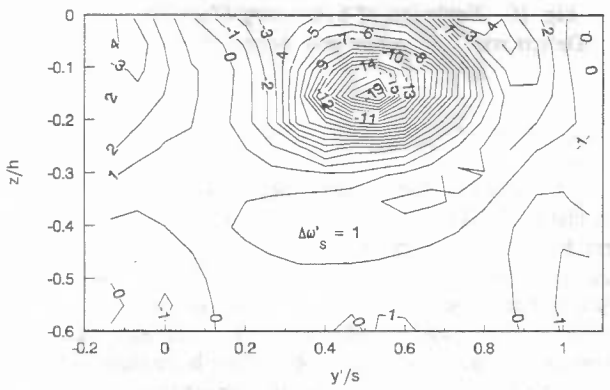

(ii) Thick inlet boundary layer.

Fig. 7b. Streamwise vorticity contours for $\tau/c = 0.055$.

The total pressure contours suggest that the losses due to the secondary and tip-leakage flows are fairly insensitive to the inlet boundary layer thickness. To quantify this observation, the overall mass-averaged total pressure coefficient was calculated for the downstream measurement plane and was divided into inlet, profile, secondary and tip-leakage components.

It should be noted that the work of Sjolander and Amrud (1987) indicated that for the present cascade, the classic horseshoe vortex separation was present, in a diminished form, for less than 1 percent clearance only. In the thick tip-wall boundary layer cases of the present work, the inlet velocity profile is fairly full, and hence the majority of the vorticity in the boundary layer is concentrated near the tip wall. On this basis, one could speculate that the observation of Sjolander and Amrud for thin inlet boundary layer should apply to the thick boundary layer tests of the present work. Tip-wall flow visualization results obtained as part of the present study seemed to confirm this.

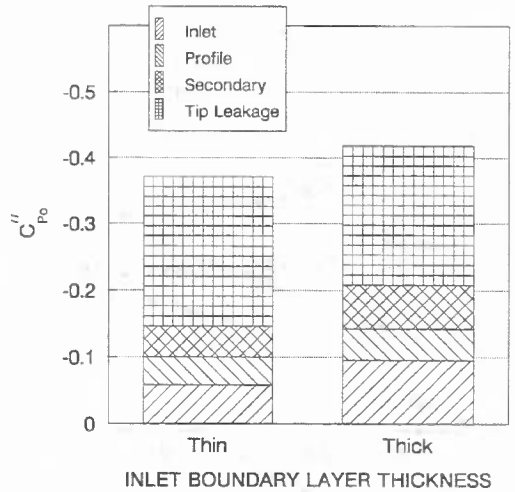

Fig. 8. Total-Pressure Coefficients for $\tau/c = 0.055$ - Variation with Inlet Boundary Layer Thickness.

The profile loss component was obtained in the same manner as for the zero clearance case. Mass averaging the total pressure deficit over the negative vorticity field provided the tip-leakage component together with the inlet deficit carried by that stream tube. Deduction of this loss and the profile loss from the overall loss resulted in the secondary loss, combined with the inlet loss convected through the passage by the secondary flow stream tube. The final step was the removal of the inlet deficit from the secondary and tip-leakage losses. This was realized by splitting the mass-averaged inlet total pressure deficit between the tip-leakage and secondary flows in proportion to the mass flow associated with each of the two flows. This approach assumes a uniform distribution of the mass-averaged inlet deficit over the cascade inlet. Since the inlet total pressure deficit is due to the wall boundary layer, its spanwise distribution is nonuniform. However, the mass flow rate is also less in the boundary layer. Therefore, the total pressure nonuniformity is considerably less pronounced when expressed in mass-weighted terms. For the thick inlet boundary layer, the total pressure deficit affects essentially the whole of the inlet streamtube, as evident from Figure 4. The resulting breakdown of the mass-averaged total pressure coefficients is given in Figure 8.

The changes in secondary and tip-leakage losses with inlet boundary layer thickness are quite small and close to the uncertainty in the data. The same measurements were taken for a clearance of 1.5 percent of the blade chord. The results supported the observations made here for the larger clearance, exhibiting even smaller changes in the tip-leakage and secondary losses with increasing boundary layer thickness.

When the tip clearance is opened, a portion of the tip-wall boundary layer is expected to enter the tip gap, as was observed by Sjolander and Amrud (1987) and Yaras et al. (1989). The amount of inlet boundary layer entering the gap is likely to depend on the boundary layer thickness and the tip-clearance

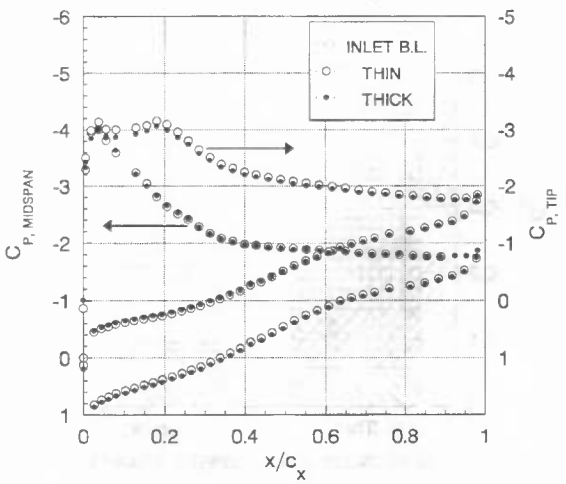

Fig. 9. Blade Loading at Midspan and 0.045h from Tip for τ/c = 0.015 - Variation with Inlet Boundary Layer Thickness.

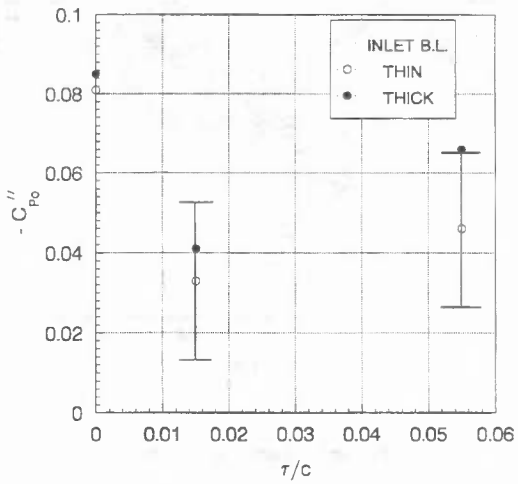

Fig. 10. Variation of Secondary-Flow Total-Pressure Deficit with Clearance and Boundary Layer Thickness.

height. In light of this, the results in Figure 8 suggest that the amount of boundary layer fluid in the tip-leakage flow has negligible impact on the tip-leakage loss.

Yaras and Sjolander (1992) found that the tip-leakage losses due to the formation and diffusion of the tip-leakage vortex were closely approximated by the leakage kinetic energy at the tip-gap exit, as given by the normal component of the gap velocity. In this context, Yaras et al. (1989) observed that the acceleration of the leakage flow into the gap is due to tip-gap pressure differences closely approximating the undisturbed blade loading at the tip. Figure 9 shows the blade pressure distribution near the tip and at midspan for thin and thick inlet boundary layers. Some unloading is evident near the tip for the increased boundary layer thickness, but it is very small. Based on this, the losses due to the formation and diffusion of the tip-leakage vortex would be expected to be essentially unchanged, which is consistent with the results in Figure 8.

The chordwise velocity component in the gap is known to depend on the streamwise momentum of the fluid entering the tip gap (Yaras et al., 1989). Hence, it is likely to be susceptible to the amount of boundary layer fluid, with relatively low streamwise momentum, which enters the tip gap. This may modify the separation "vortex" structure on the blade tip, hence altering the entropy generated within the tip gap. However, this should not affect the tip-leakage losses significantly since the losses within the gap itself account for a relatively small proportion of the overall tip-leakage losses (Yaras and Sjolander, 1992).

Figure 8 shows only a small change in secondary losses with increasing inlet boundary layer thickness. For 1.5 percent clearance size this change in secondary losses was even smaller. These results are in agreement with the observations for zero clearance (Figure 6) where the amount of inlet boundary layer fluid involved in secondary flows did not alter the secondary losses.

The variation of secondary losses with clearance size is shown in Figure 10. The error bands shown for the thin boundary layer results represent a very conservative estimate of the uncertainty in the data. Even when the uncertainty is taken into account, there is a distinct reduction in the secondary losses as the tip gap is opened. As was stated earlier, for nonzero clearances a significant portion of the inlet boundary layer fluid is known to enter the tip gap, and hence the tip-leakage vortex. This implies that reduced amounts of the inlet boundary layer fluid are convected through the passage by the secondary flow. However, comparison of the secondary losses for thin and thick inlet boundary layers has already indicated that the amount of boundary layer fluid entering the secondary flows has little influence on the secondary losses. The observed trend in the secondary losses with clearance is more likely to stem from changes in the dominant secondary-loss generation mechanisms as the tip clearance is opened.

In the previous section, the "new" endwall boundary layer developing within and downstream of the blade passage was stated to be an important source of secondary losses for zero tip clearance. However, when the tip gap is opened the development of a substantial portion of this endwall boundary layer is primarily influenced by the velocity and pressure distribution in the leakage jet and the tip-leakage vortex. As the leakage flow enters the tip gap a new boundary layer starts at the dividing stream surface shown in Figure 11. This boundary layer grows until it reaches the separation line, S_1, at which point the boundary layer fluid is lifted off the wall and much of it becomes part of the tip-leakage vortex. The downstream measurements of Yaras and Sjolander (1989) showed that the loss generated by this endwall boundary scales on the leakage kinetic energy at the gap exit and the tip-leakage loss model proposed by Yaras and Sjolander (1992) seems

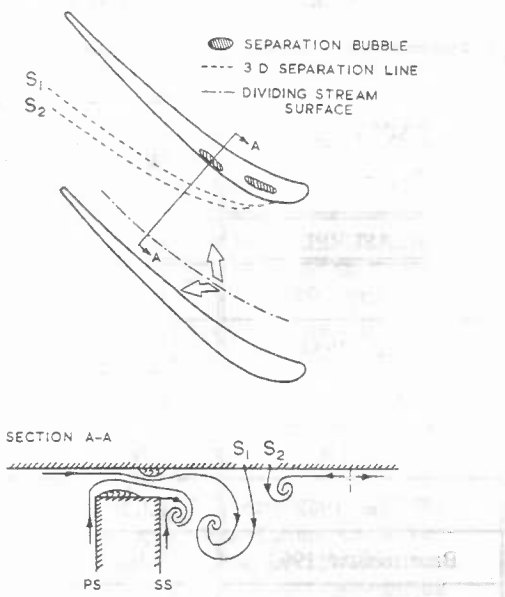

Fig. 11. Interpretation of Tip-Gap Flow Structures (from Sjolander and Amrud, 1987).

to account for this loss component implicitly. With a large portion of the endwall boundary layer loss within and downstream of the blade passage now included in the tip-leakage losses, a substantial reduction in the secondary losses is expected.

For zero clearance another significant mechanism for secondary-loss generation is the viscous dissipation in the passage vortex. As evident in Figure 7(b), for nonzero clearances the passage vortex is pushed a considerable distance away from the suction side of the passage by the tip-leakage vortex. This is likely to alter the cross-stream pressure gradients experienced by the passage vortex. It is plausible that this together with the shear interaction between the counter rotating tip-leakage and passage vortices may reduce the amount of secondary kinetic energy associated with the passage vortex. The dissipation within the passage vortex would consequently be lessened.

From Figure 10, after the initial drop in secondary losses when the tip gap is opened, there appears to be a slight rise with increasing clearance size. However, as indicated in the figure, the rise is well within the uncertainty in the data and may not be genuine. Based on the present limited data it is possible to assert only that there was a noticeable reduction in the secondary losses as the gap was opened.

Prediction of Endlosses

Yaras and Sjolander (1992) developed an endloss model for nonzero tip clearance of the form

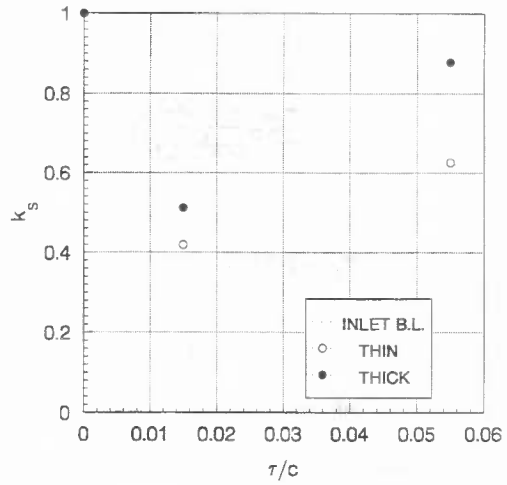

Fig. 12. Variation of Secondary-Flow Correction Factor, k_S, with Tip Clearance.

$$Y_{end} = Y_{gap} + Y_{tip} + k_s Y_{s,0} \tag{5}$$

where k_s is the fraction of zero-clearance secondary loss that is identifiably associated with the secondary flow structure for nonzero tip clearance. Y_{gap} is the loss inside the tip gap itself, Y_{tip} is the loss associated with the tip-leakage flow downstream of the gap, and $Y_{s,0}$ is the secondary loss at zero clearance. In traditional loss systems k_S is implicitly assumed to be 1.0.

The loss components in equation (5) correspond to fully mixed-out conditions downstream of the cascade. The mixing losses downstream of the current measurement plane were calculated by applying the conservation equations to a mixing process at constant area between the measurement plane and a completely mixed-out downstream flow. Comparison between the overall mass-averaged loss in the measurement plane and the fully mixed-out loss showed that the majority of the mixing loss occurs prior to the measurement plane. This enabled the values of k_s to be calculated on the basis of the mass-averaged secondary losses obtained from the measurement plane.

The current study suggests that the thickness of the inlet boundary layer has little effect on the secondary losses, regardless of the clearance size. Thus, k_s may not be affected by the boundary layer thickness at the inlet. The results in Figure 10 show a substantial reduction in the secondary losses with the opening of the tip gap, the amount of reduction being dependent on the tip-gap size. This implies a dependence of k_s on the clearance size, as shown in Figure 12. It is clear that the traditional approach which ignores the interaction between the tip-leakage and secondary loss mechanisms, may be very misleading.

For the losses generated inside the tip gap and during the mixing of the tip leakage with the main stream, Yaras and Sjolander (1992) developed the following expressions:

$$Y_{gap} = CK_G \frac{\sigma C_D C_L^{1/2}}{\cos\alpha_m}\left(\frac{c}{h}\right) \quad (6)$$

$$Y_{tip} = 2K_E\sigma\frac{\tau}{h}C_D\frac{\cos^2(\alpha_2)}{\cos^3(\alpha_m)}C_L^{1.5} \quad (7)$$

where

$$\sigma = \frac{c}{S} \quad , \quad C_D = 0.75 \quad , \quad C = 0.007$$

and

$$K_E = 0.566, \quad K_G = 0.943$$

for front- or aft-loaded blades;

$$K_E = 0.5, \quad K_G = 1.0$$

for mid-loaded blades. These expressions appear to be satisfactory on the basis of the present data.

To identify an appropriate correlation for $Y_{s,0}$, the zero clearance secondary losses from the present study are compared in Table 2 with various secondary-loss correlations available in the published literature. None of the correlations agrees exactly with the experimental data. However, the correlation of Kacker and Okapuu (1982) appears as good as any of them and is thus recommended for use in the endloss model of Yaras and Sjolander.

As evident from the discussion in the previous section, the interaction between the tip-leakage and secondary flows is very complex and it is unlikely that clearance size is the only parameter affecting the value of k_s. More experimental work is required to establish the dependence of k_s on parameters such as inlet boundary layer skew, blade loading and flow turning, which are known to influence both the tip-leakage and secondary loss generation mechanisms. It would also be highly desirable to repeat the measurements for a blade row with higher turning, and thus stronger secondary flows, as is more typical of turbines. Furthermore, the work of Yaras et al. (1992) in a turbine cascade showed that relative wall motion in turbines reduces the tip-leakage vortex size substantially while the passage vortex is enhanced by the scraping effect of the blades on the tip-wall boundary layer. Thus all three loss components in equation (5) are expected to be altered by the relative wall motion. These effects are yet to be modelled.

CONCLUSIONS

The present study has attempted to clarify the interaction between the tip-leakage and secondary flows and the influence of the inlet boundary thickness.

The secondary losses generated within and downstream of the blade passage were found to be insensitive to the boundary layer thickness at the inlet for both zero and nonzero clearances.

Table 2. Comparison Between Measured Secondary Losses (Zero Clearance) and Various Correlations (from Dunham, 1970 and Sieverding, 1985).

SOURCE	$Y_{s,0}$	
	THIN INLET BOUNDARY LAYER	THICK INLET BOUNDARY LAYER
MEASURED	0.050	0.059
Soderberg, 1949	0.092	0.092
Ehrich, 1954	0.043	0.043
Scholz, 1954	0.085	0.085
Vavra, 1960	0.065	0.065
Boulter, 1962	0.028	0.028
Bauermeister, 1963	0.162	0.162
Dunham, 1970	0.027	0.039
Kacker and Okapuu, 1982	0.068	0.068

Likewise, the tip-leakage losses remained essentially unchanged as the inlet boundary layer thickness was varied.

In contrast to the assumption made in most loss systems, the secondary losses were found to be significantly influenced by the tip-gap size. For typical values of clearance, a reduction in the losses of the order of 50 percent was found. Physical arguments based on the observed flow behaviour were presented to account for this reduction.

The endloss model of Yaras and Sjolander (1992) was reviewed in light of the present findings. The present data allow approximate values to be assigned to the secondary loss correction factor, k_s, which had been postulated in the earlier paper. At this point, only the dependence of k_s on the clearance size has been estimated. The influence of other factors, such as relative wall motion in particular, remains to be established.

ACKNOWLEDGEMENTS

Financial support for this study provided by the Natural Sciences and Engineering Research Council of Canada under Grant A1671 and by Pratt & Whitney Canada Inc. is gratefully acknowledged.

REFERENCES

Denton, J.D., 1993, "Loss Mechanisms in Turbomachines," ASME Journal of Turbomachinery, Vol. 115, pp. 621-656.

Dishart, P.T. and Moore, J., 1990, "Tip Leakage Losses in a near Turbine Cascade," ASME Journal of Turbomachinery, Vol. 2, pp. 599-608.

Dunham, J., 1970, "A Review of Cascade Data on Secondary osses in Turbines," Journal of Mechanical Engineering Sciences, ol. 12, No. 1, pp. 48-59.

Dunham, J. and Came, P.M., 1970, "Improvements to the inley-Mathieson Method of Turbine Performance Prediction," SME Journal of Engineering for Power, Vol. 92, No. 3, pp. 252-56.

Gregory-Smith, D.G., 1982, "Secondary Flows and Losses in xial-Flow Turbines," ASME Journal of Engineering for Power, ol. 104, pp. 819-822.

Kacker, S.C. and Okapuu, U., 1982, "A Mean Line Prediction Method for Axial Flow Turbine Efficiency," ASME Journal of Engineering for Power, Vol. 104, pp. 111-119.

Rodger, P. Sjolander, S.A. and Moustapha, S.H., 1992, Establishing Two-Dimensional Flow in a Large-Scale Planar Turbine Cascade," AIAA Paper 92-3066.

Sharma, O.P. and Butler, T.L., 1987, "Predictions of Endwall Losses and Secondary Flows in Axial Flow Turbine Cascades," ASME Journal of Turbomachinery, Vol. 109, pp. 229-236.

Sieverding, C. H., 1985, "Recent Progress in the Understanding of Basic Aspects of Secondary Flows in Turbine Blade Passages," ASME Journal of Engineering for Gas Turbines and Power, Vol. 107, pp. 249-257.

Sjolander, S.A. and Amrud, K.K., 1987, "Effects of Tip Clearance on Blade Loading in a Planar Cascade of Turbine Blades," ASME Journal of Turbomachinery, Vol. 109, pp. 237-245.

Yamamoto, A., 1988, "Interaction Mechanisms Between Tip Leakage Flow and the Passage Vortex in a Linear Turbine Rotor Cascade," ASME Journal of Turbomachinery, Vol. 110, pp. 329-338.

Yaras, M.I. and Sjolander, S.A., 1989, "Losses in the Tip Leakage Flow of a Planar Cascade of Turbine Blades," AGARD-CP-469, "Secondary Flows in Turbomachines," Paper 20.

Yaras, M.I. and Sjolander, S.A., 1990, "Development of the Tip-Leakage Flow Downstream of a Planar Cascade of Turbine Blades: Vorticity Field," ASME Journal of Turbomachinery, Vol. 112, pp. 609-617.

Yaras, M.I. and Sjolander, S.A., 1992, "Prediction of Tip-Leakage Losses in Axial Turbines," ASME Journal of Turbomachinery, Vol. 114, pp. 204-210.

Yaras, M.I., Sjolander, S.A. and Kind, R.J. 1992, "Effects of Simulated Rotation on Tip Leakage in a Planar cascade of Turbine Blades Part II: Downstream Flow Field and Blade Loading," ASME Journal of Turbomachinery, Vol. 114, pp. 660-667.

Yaras, M.I., Zhu, Y. and Sjolander, S.A., 1989, "Flow Field in the Tip Gap of a Planar Cascade of Turbine Blades," ASME Journal of Turbomachinery, Vol. 111, pp. 276-283.